Complete Structure of the Cell Surface Polysaccharide of *Streptococcus oralis* ATCC 10557: A Receptor for Lectin-Mediated Interbacterial Adherence†

Chitrananda Abeygunawardana and C. Allen Bush*

Department of Chemistry and Biochemistry, University of Maryland, Baltimore County, Baltimore, Maryland 21228

John O. Cisar

Laboratory of Microbial Ecology, National Institute of Dental Research, Bethesda, Maryland 20892

Received February 8, 1991; Revised Manuscript Received April 1, 1991

ABSTRACT: Lectin–carbohydrate binding is known to play an important role in a number of different cell–cell interactions including those between certain species of oral streptococci and actinomyces that colonize teeth. The cell wall polysaccharides of *Streptococcus oralis* ATCC 10557, *S. oralis* 34, and *Streptococcus mitis* J22, although not identical antigenically, each function as a receptor molecule for the galactose and *N*-acetylgalactosamine reactive fimbrial lectins of *Actinomyces viscosus* and *Actinomyces naeslundii*. Carbohydrate analysis of the receptor polysaccharide isolated from *S. oralis* ATCC 10557 shows galactose (3 mol), glucose (1 mol), GalNAc (1 mol), and rhamnose (1 mol). ^{1}H NMR spectra of the polysaccharide show that is is partially O-acetylated. Analysis of the ^{1}H NMR spectrum of the de-O-acetylated polysaccharide shows that it is composed of repeating subunits containing six monosaccharides and that the subunits are joined by a phosphodiester linkage. The ^{1}H and ^{13}C NMR spectra were completely assigned by two-dimensional homonuclear correlation methods and by ^{1}H-detected heteronuclear multiple-quantum correlation (^{1}H[^{13}C]HMQC). The linkage of the component monosaccharides in the polymer, deduced from two-dimensional ^{1}H-detected heteronuclear multiple-bond correlation spectra (^{1}H[^{13}C]HMBC), shows that the repeating unit of the de-O-acetylated polymer is a linear hexasaccharide with no branch points. The complete ^{1}H and ^{13}C assignment of the native polysaccharide was carried out by the same techniques augmented by a ^{13}C-coupled hybrid HMQC-COSY method, which is shown to be especially useful for carbohydrates in which strong coupling and overlapping peaks in the ^{1}H spectrum pose difficulties. The fully assigned spectra of the native polymer show that each of two different positions is acetylated in one-third of the repeating subunits and that the acetylation is randomly distributed along the polymer. The exact positions of acetylation were assigned by a carbonyl-selective HMBC method that unambiguously defines the positions of O-acetylation. The complete structure of the native polysaccharide in *S. oralis* ATCC 10557 is

$$[\rightarrow 6)\mathrm{Gal}_p(\alpha 1\rightarrow 3)\mathrm{Rha}_p(\beta 1\rightarrow 4)\mathrm{Glc}_p(\beta 1\rightarrow 3)\mathrm{Gal}_f(\beta 1\rightarrow 6)\mathrm{Gal}_p(\beta 1\rightarrow 3)\mathrm{Gal}_p\mathrm{NAc}(\alpha 1\rightarrow \mathrm{PO}_4^-)]_n$$

with $(OAc)_{0.33}$ at position 2 and $(OAc)_{0.33}$ at position 6.

Comparison of this structure with those previously determined for the polysaccharides of strains 34 and J22 suggests that the similar lectin receptor activities of these molecules may depend on internal galactofuranose linked (β1→6)- to Gal(β1→3)GalNAc(α) or GalNAc(β1→3)Gal(α).

The carbohydrates of glycoproteins, glycolipids, proteoglycans, and bacterial polysaccharides have very complex structures, which are often branched and feature highly varied chemical functionality. Their biosynthesis requires a host of specific glycosyl transferases and processing enzymes at a considerable expense of biochemical free energy. It has been proposed that these biopolymers are informational macromolecules in whose structure is encoded signals that are crucial for biological functions related to intercellular communication and control of cellular growth and differentiation. The mechanism for decoding the information stored in complex carbohydrates depends on their binding with lectins. Although the presence of lectins in plants has been recognized for some time, it has been only recently discovered that they are widely distributed in animal tissues in small quantities (Drickamer, 1988).

Lectins also occur on the surfaces of many bacteria and function to mediate adherence by binding to the carbohydrates of glycoproteins and glycolipids of animal cell surfaces. Bacterial lectins also have been detected that bind to polysaccharides on other bacterial species resulting in coaggregation. These lectin-mediated interactions between different bacteria have been demonstrated extensively among members of the human oral flora and are thought to contribute to the formation of mixed microbial communities on teeth (Cisar et al., 1985) as well as other oral tissue surfaces (Hughes et al., 1988).

This possibility was initially revealed by the lactose-sensitive coaggregation between *Actinomyces viscosus* T14V and *Streptococcus oralis* 34[1] (McIntire et al., 1978), two Gram-

† A preliminary account of this investigation was presented at the 18th Meeting of the Society for Complex Carbohydrates, Ann Arbor, MI, Nov 8–11, 1989. For the abstract of this presentation, see Abeygunawardana, C., and Bush, C. A. (1989) *Glycoconjugate J. 6*, 425. Research supported by NIH Grant DE-09445.

* To whom correspondence should be addressed.

0006-2960/91/0430-6528$02.50/0

positive species that are closely associated in dental plaque. Subsequent studies attributed the similar cell surface lectin activities of various *A. viscosus* and *Actinomyces naeslundii* strains to the presence of type 2 fimbriae on these bacteria (Cisar, 1986) and the receptor activity of *S. oralis* 34 to a cell wall polysaccharide having the following structure (Abeygunawardana et al., 1989):

$$[\rightarrow 6)Gal_pNAc(\alpha 1\rightarrow 3)Rha_p(\beta 1\rightarrow 4)Glc_p(\beta 1\rightarrow 6)Gal_f(\beta 1\rightarrow 6)Gal_pNAc(\beta 1\rightarrow 3)Gal_p(\alpha 1\rightarrow PO_4^-\text{-}]_n$$

The GalNAc(β1→3)Gal moiety of the hexasaccharide subunit was proposed to be the site of lectin binding on the basis of the inhibition of coaggregation by this disaccharide (McIntire et al., 1988) as well as the attachment of radiolabeled *A. naeslundii* to globoside, a glycolipid with terminal GalNAc(β→3)Gal, on thin-layer chromatograms (Brennan et al., 1987). Significantly, antibody reactivity with the strain 34 polysaccharide was not inhibited by GalNAc(β1→3)-Galα-OMe but instead appeared to be directed against the α-linked GalNAc end of the hexasaccharide subunit (McIntire et al., 1988). The apparent difference in antigenic and bacterial lectin receptor structures provided a possible explanation for the expression of similar receptor activities by other serologically distinct streptococcal strains such as *Streptococcus mitis* J22. Isolation of the J22 cell wall polysaccharide and structural analysis using high-resolution NMR revealed the following structure (Abeygunawardana et al., 1990):

$$[\rightarrow 6)Gal_pNAc(\alpha 1\rightarrow 3)Rha_p(\beta 1\rightarrow 4)Glc_p(\beta 1\rightarrow 6)Gal_f(\beta 1\rightarrow 6)\text{-}Rha(\alpha 1\rightarrow 2)\text{-}\nearrow Gal_p(\beta 1\rightarrow 3)Gal_pNAc(\alpha 1\rightarrow PO_4^-\text{-}]_n$$

Like GalNAc(β1→3)Gal in the *S. oralis* 34 polysaccharide, Gal(β1→3)GalNAc in the *S. mitis* J22 polysaccharide was previously shown to be a potent inhibitor of lectin-mediated coaggregation (McIntire et al., 1983). Moreover, Gal(β1→3)GalNAc containing glycoconjugates were identified as potential receptors for the attachment of *A. naeslundii* to sialidase-treated epithelial cells (Brennan et al., 1986, 1987) and of *A. viscosus* to sialidase-treated glycoprotein-coated latex beads (Heeb et al., 1985).

Streptococcus oralis ATCC 10557 was isolated from a patient with subacute bacterial endocarditis, and, like strains 34 and J22, this organism participates in lectin-mediated coaggregations with representative *Actinomyces* strains (Sato et al., 1984). The cell wall polysaccharide of strain 10557 was previously shown to contain GalNAc, Gal, Rha, and Glc along with some phosphate (Koga et al., 1983) and also was found to inhibit the lactose-sensitive coaggregations of strain 10557 with *A. viscosus* 19246 (Sato et al., 1984) and of *S. oralis* 34 with *A. viscosus* T14V (McIntire et al., 1988). In spite of their similar inhibitory activities, antiserum against strain 34 failed to react with the 10557 polysaccharide. To further explore the lectin receptor and antigenic properties of streptococcal polysaccharides, the structure of the *S. oralis* ATCC 10557 polysaccharide was determined by high-resolution NMR.

Materials and Methods

The cell wall polysaccharide of *S. oralis* ATCC 10557 was isolated by methods similar to those previously described for the receptor polysaccharide of *S. mitis* J22 (Abeygunawardana et al., 1990). This involved the preparation of cell walls from bacteria grown in complex media, digestion of the cell walls with mutanolysin (M-3765, Sigma Chemical Co., St. Louis, MO), precipitation of protein in the presence of cold 5% trichloroacetic acid, and purification of the receptor polysaccharide from the neutralized soluble fraction by anion-exchange and gel-filtration column chromatography. Fractions were assayed for carbohydrate by the phenol–sulfuric acid method (Dubois et al., 1956) and for lectin receptor activity by an inhibition of hemagglutination assay using the lectin of *Bauhinia purpurea* (L-2501, E.Y. Labs, Inc., San Mateo, CA or Sigma L-6013) and human O erythrocytes. The elution profile of the 10557 receptor polysaccharide from (diethylaminoethyl)cellulose (DE52, Whatman, Inc., Clifton, NJ) was like that described for the polysaccharide of strain J22 (Abeygunawardana et al., 1990). When applied to a calibrated column of Sephacryl S-400 (Pharmacia) in a 0.1 M NaCl, 0.01 M Tris HCl buffer (pH 7.6), the 10557 polysaccharide emerged at a position similar to that of a clinical dextran (Sigma D4751) with average molecular mass of 80 kDa determined by light scattering. The 10557 polysaccharide gave a reaction of complete identity with a sample of the previously studied ATCC 10557 serotype II carbohydrate antigen (Koga et al., 1983) kindly provided by Dr. S. Hamada (Osaka University, Suita-Osaka, Japan).

Sugar Composition. The carbohydrate composition of the polysaccharide samples was determined by HPLC of the perbenzoylated methyl glycosides according to the method of Jentoft (1985). Polysaccharide sample (2 mg) was depolymerized with 0.5 mL of 48% HF at 4 °C for 24 h. After removal of HF under vacuum (with a NaOH column protecting the pump), the sample was redissolved in 0.5 mL of water and lyophilized. Constituent sugars were converted to perbenzoylated methyl glycosides as described earlier (Abeygunawardana et al., 1990). The peaks in the HPLC chromatograms were assigned from the retention times of perbenzoylated methyl glycoside samples prepared from the corresponding pyranosides.

De-O-acetylation. Polysaccharide (20 mg) was dissolved in 2 mL of dilute ammonia (pH 11.0) and was kept at 4 °C for 24 h. Excess ammonia was removed by flushing with nitrogen, and the solution was lyophilized.

Partial Acid Hydrolysis. Another sample of de-O-acetylated polysaccharide (15 mg) was passed through a Dowex 50W-X8 column (1 × 20 cm) and lyophilized. The dried sample was dissolved in 0.5 mL of D_2O (pD 1.9) and heated at 80 °C in the NMR probe. The hydrolysis reaction was monitored for 3–4 h by the disappearance of the α-glycosyl phosphate resonance at 5.480 ppm in the ^1H NMR spectrum. Fractionation of products by gel filtration with BioGel P-6 and water as eluent indicated that the hydrolysis reaction cleaved the glycosyl phosphate linkage nearly quantitatively. The void fraction, which contained <5% of the total carbohydrates, appeared to contain mainly higher oligomers of the repeating unit and peptidoglycan fragments representing the linkage to the bacterial cell wall (Abeygunawardana and Bush, unpublished results). Further characterization of the oligosaccharides indicated that the hydrolysis produced a major oligosaccharide (hexasaccharide) representing the repeating unit in the polymer together with two minor oligosaccharides (a tetra- and a disaccharide) that result from partial hydrolysis of the hexasaccharide units rather than being minor components in the polysaccharide (Abeygunawardana et al., manuscript in preparation).

Nuclear Magnetic Resonance Spectroscopy. Spectra were recorded on a GE GN-500 (500.11-MHz ^1H), a Bruker AM-500 (550.11-MHz ^1H), a Bruker AM-600 (600.13-MHz ^1H),

[1] *Streptococcus sanguis* strains ATCC 10557, 34, and J22 have been designated as *S. oralis* ATCC 10557, *S. oralis* 34, and *S. mitis* J22, respectively, based on the taxonomic scheme of Kilian et al. (1989).

and a Nicolet NT-300 (300.06-MHz ^1H) spectrometer. The observed ^1H chemical shifts are reported relative to internal sodium 4,4-dimethyl-4-silapentane-1-sulfonate (DSS) with acetone as an internal standard (2.225 ppm downfield from DSS). The carbon chemical shifts are determined relative to internal acetone (31.07 ppm). The phosphorus chemical shifts are reported relative to the external reference signal of 85% H_3PO_4 contained in a sealed capillary tube. Polysaccharide samples (20 mg) were exchanged three times in D_2O (99.8 atom % *d*) followed by lyophilization. The final solution was prepared by dissolving the sample in high purity (99.96 atom % *d*) D_2O (Merck, Sharp & Dohme Co.).

2D NMR data were collected without sample spinning at 25 °C. Pulse sequences and parameters used to collect 2D NMR data are described below. Processing parameters and additional experimental details are given in the figure captions. 2D ^1H–^1H correlation spectra at 500 MHz were obtained by the standard pulse sequence (Rance et al., 1983), which allowed for coherence transfer through a double-quantum filter (DQF-COSY). Two sets of 386 × 1024 data points were acquired in adjacent blocks of memory, and the data were processed by the method of States et al. (1982). Phase-sensitive homonuclear Hartmann–Hahn (HOHAHA) spectra (Braunschweiler & Ernst, 1983; Davis & Bax, 1985) at 500 MHz were obtained with isotropic mixing by the MLEV 17 method using the pulse sequence of Bax and Davis (1985). The total spin-lock mixing time was 72 ms, and a 1.5-s relaxation delay was used with a 34-μs 90° pulse and a 2-ms trim pulse. Phase-sensitive 2D NOESY spectra at 500 MHz were acquired and processed by the method of States et al. (1982). Phase-sensitive triple-quantum filtered COSY (Piantini et al., 1982) spectra (TQF-COSY) at 500 MHz were recorded with the pulse sequence $90°$–t_1–$90°_{\phi}90°_{\phi'}$–$90°_{\psi}90°_{\psi'}$–acq with composite pulses (Muller et al., 1986). Exchangeable amide protons of acetamido sugars in native polysaccharide (15 mg) were observed in a 90:10 mixture of H_2O and D_2O with 0.01 M trifluoroacetic acid at 300 MHz by selective excitation with the Redfield 2–1–4–1–2 pulse sequence (Redfield, 1978). Acetamido proton resonances were assigned from DQF-COSY spectra (data not shown) at 300 MHz recorded in the same solvent with presaturation of water signal by low-power irradiation during the 3-s relaxation delay.

Broad-band ^1H-decoupled ^{13}C spectra were obtained at 75 MHz with a 15-kHz spectral width and 16K complex data points. The 90° ^{13}C pulse length was 12 μs, and MLEV 16 decoupling was used (Levitt et al., 1982). DEPT spectra (Doddrell et al., 1982) were obtained with broad-band ^1H decoupling, a 135° ^1H pulse (115.5 μs), and a 3.4-ms delay chosen to equal $1/(2 \times {}^1J_{CH})$ between pulses. ^1H–^{13}C single-bond correlation spectra were collected in the proton-detected mode with Bruker 5-mm inverse broad-band probe using Bruker reverse electronics. The pulse sequence used for the single-bond ^1H–^{13}C heteronuclear multiple-quantum correlation ($^1H[^{13}C]$HMQC) experiments was that of Bax et al. (1983). WALTZ-16 (Shaka et al., 1983) decoupling at the carbon frequency was used during acquisition to collapse proton–carbon couplings.

All other heteronuclear correlation data were collected with a 5-mm RPT probe. Hetero nuclei were pulsed with X-nucleus decoupling hardware in the GN-500 spectrometer. A 32-μs ^{13}C pulse width was used in all the experiments. Modified phase cycling was used for phase-sensitive data acquisition by the method of States et al. (1982). The ^{13}C frequency was set approximately at 64 ppm with a sweep width of 12 500 Hz. Typically, 2 × 256 × 1024 data sets were collected and zero filled in the t_1 dimension to give a final data matrix of 1K × 1K real points. Digital resolution in that ^{13}C and ^1H dimensions are ±0.1 and ±0.005 ppm/point, respectively. A combination experiment (HMQC-COSY) of ^1H-detected heteronuclear multiple-quantum coherence (HMQC) with homonuclear correlated (COSY) experiment (Gronenborn et al., 1989) was carried out without ^{13}C decoupling during the acquisition. A total of 112 scans were collected for each t_1 value preceded by four dummy scans. The total experimental time was 36 h. ^1H-detected heteronuclear multiple-bond correlation spectra (Bax & Summers, 1986) were recorded in the phase-sensitive mode (Bax & Marion, 1988) without ^{13}C decoupling during the acquisition. Delays of 3.4 ms [$1/(2 \times {}^1J_{CH})$] and 60 ms [$<1/{}^nJ_{CH}$] were used with a 1.5-s relaxation delay between acquisitions. Typically, 48–64 scans were collected for each t_1 value, preceded by two dummy scans. Another HMBC data set was recorded for the native polysaccharide by using the pulse sequence described above, with all ^{13}C pulses being semiselective (90° pulse = 285 μs). The ^{13}C frequency was set at the carbonyl carbon region (≈178 ppm) with a sweep width of 1000 Hz. A total of 2 × 32 × 1024 complex data points were acquired with 512 scans per t_1 value.

All NMR data processing was carried out on VAX Station 3200 and personal Iris computers using the FTNMR program (Hare Research Inc., Woodinville, WA). GN data were transferred via Ethernet to these computers and converted to "readable" files by an in-house program (GENET). Bruker data sets were transferred to the VAX via magnetic tape and the Bruker data transfer protocol in the FTNMR program.

RESULTS

The ^1H NMR spectrum of *S. oralis* ATCC 10557 polysaccharide, hereafter referred to as the native polysaccharide, in D_2O at 600 MHz (data not shown) shows a complicated anomeric proton region having multiple peaks with different intensities. It also showed a quartet at 5.481 ppm indicating an anomeric proton of an α-glycosyl phosphate residue. The spectrum contains several upfield methyl resonances at 1.343 (d, J = 5.5 Hz) and 2.045 (s) ppm and two singlets at 2.138 and 2.141 ppm indicating the presence of a 6-deoxyhexose, an acetamido sugar, and two O-acetate substituents in the repeating unit. The presence of an acetamido sugar residue was confirmed by the amide proton resonance at 8.207 ppm in the ^1H NMR spectrum in H_2O. Each of the O-acetate methyl groups has $^1/_3$ of the intensity of the acetamido methyl group.

Carbohydrate analysis by reverse-phase HPLC of the benzoylated methyl glycosides of the polysaccharide showed 3 mol of Gal and 1 mol each of GalNAc, Glc, and Rha. In contrast to the low phosphorus content reported for the polysaccharide from the same strain reported by Koga et al. (1983), our ^1H and 202 MHz ^{31}P NMR data (single ^{31}P resonance at –0.67 ppm, pD 7.0) suggest the presence of a phosphodiester linkage (teichoic acid type) in the polymer. The ^1H NMR spectrum of the polysaccharide sample prepared by removal of O-acetate groups with dilute ammonia, hereafter referred to as the de-O-acetylated polymer, shows six anomeric resonances and a complete absence of signals at 2.14 ppm. The hexasaccharide obtained from mild acid hydrolysis of the de-O-acetylated polymer shows a single phosphate resonance at 1.13 ppm (pD 1.9). The ^1H NMR spectrum of the hexasaccharide (data not shown) shows eight anomeric resonances, including two assigned to the α- and β-anomers of reducing terminal sugar and the two anomeric resonances for the next sugar unit. The absence of a proton resonance at 5.481 ppm

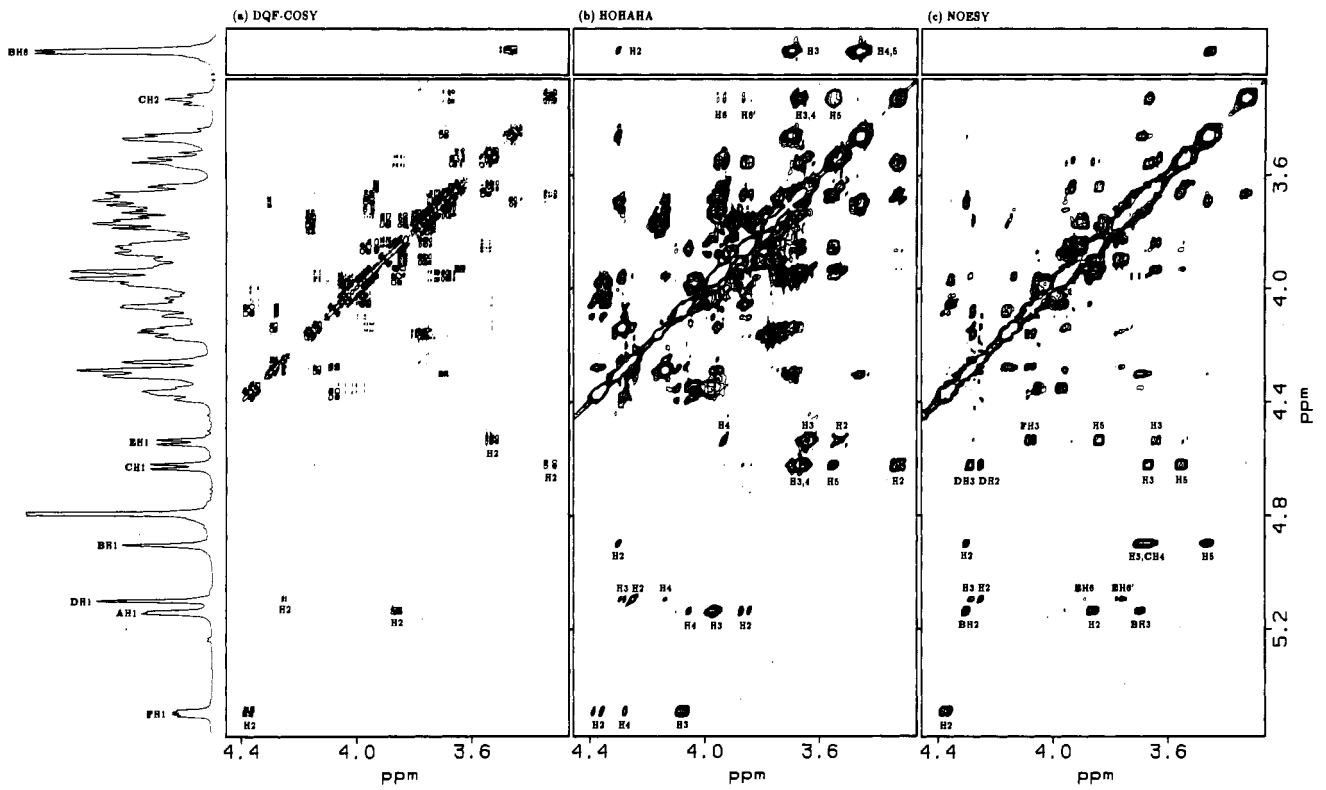

FIGURE 1: ^{1}H homonuclear two-dimensional correlation spectra of the de-O-acetylated polysaccharide from *S. oralis* ATCC 10557 at 500 MHz. (a) DQF-COSY spectrum. The data matrix was 2 × 400 × 1K complex points with 32 scans per t_1 value. Sine bell apodization with 20° and 30° phase shifts were used in the t_2 and t_1 dimension, respectively. Positive and negative contours are plotted with different line thicknesses. (b) HOHAHA spectrum (72-ms spin-lock time) and (c) NOESY spectrum (400-ms mixing time). Data matrices were 2 × 256 × 1K complex points with 8 scans per t_1 value. Gaussian line broadening (3 Hz) in the t_2 dimension and a shifted sine bell (60°) in the t_1 dimension were used prior to the Fourier transformation. All spectra were zero filled in the t_1 dimension to obtain 1K × 1K (real) matrices with a digital resolution of ±0.005 ppm/pt. The normal 1D spectrum is displayed at left.

in the ^{1}H NMR spectrum of the hexasaccharide indicated cleavage of glycosyl phosphate linkage during the mild acid hydrolysis. These data indicated that the polysaccharide from *S. oralis* ATCC 10557 is composed of a hexasaccharide repeating unit polymerized through phosphodiester linkages and that the hexasaccharide repeating unit consists of 3 mol of Gal and 1 mol each of Glc, GalNAc, Rha and phosphate and 0.33 mol each of two O-acetate substituents.

De-O-acetylated Polysaccharide. The ^{1}H NMR spectrum at 500 MHz shows six anomeric resonances at 5.481 ($J_{1,2}$ = 3.5, J_{PH} = 7 Hz), 5.126 ($J_{1,2}$ = 3.5 Hz), 5.086 ($J_{1,2}$ < 2 Hz), 4.888 ($J_{1,2}$ < 2 Hz), 4.614 ($J_{1,2}$ = 8.0 Hz) and 4.528 ($J_{1,2}$ = 8.0 Hz) ppm. Starting from these well-separated anomeric resonances, spin systems for individual sugar residues can be identified by tracing cross-peak connectivities in the DQF-COSY contour map. As discussed earlier (Abeygunawardana et al., 1990), coupling constant information obtained from the cross peaks can be utilized to assign the anomeric configuration as well as the relative stereochemistry of the particular sugar residue.

Cross-peak connectivities from the most downfield anomeric resonance (5.481 ppm) yielded proton assignment up to the H4 resonance. Cross-peak fine structure shows both H1/H2 and H3/H4 cross peaks in the DQF-COSY spectrum (Figure 1a), which has small active couplings ($J_{1,2}$ = $J_{3,4}$ = 3.5 Hz), indicating a sugar residue having the α-galactopyranosyl configuration. Since the amide resonance (8.207 ppm) showed a cross peak to H2 of this residue (4.365 ppm) in the DQF-COSY spectrum recorded in H_2O (data not shown), the identity of the residue was established as α-GalNAc. The H1/H2 cross peak for this residue (**F**) shows displacement resonance peaks in ω_1 and ω_2 cross sections due to passive long-range coupling of ^{31}P (−0.67 ppm, pD 7.0) to both proton resonances ($^3J_{PH1}$ = 7.0 and $^4J_{PH2}$ < 2.5 Hz). Similar effects have been observed previously in the DQF COSY spectrum of *S. mitis* J22 polysaccharide for α-GalNAc-1-phosphate residue (Abeygunawardana et al., 1990). The H4/H5 cross peak was not observed in the DQF-COSY spectra due to the small coupling between H4 and H5 resonances of sugars having the galactopyranose configuration ($J_{4,5}$ < 0.5 Hz).

Starting with the anomeric resonance at 5.126 ppm, resonances up to H4 of residue A were assigned in the DQF-COSY spectrum. Small active coupling constants in the H1/H2 and H3/H4 cross peaks and the absence of the H4/H5 cross peak indicate the residue to be an α-galactopyranoside. The spin system starting with the anomeric resonance at 4.528 ppm, on the other hand, showed similar behavior except for a large active coupling in the H1/H2 cross peak ($J_{1,2}$ = 8 Hz), indicating a β-galactopyranoside residue (**E**). Assignment of H5 and H6 resonances of these residues were obtained by TQF-COSY (Figure 2) discussed below.

The anomeric resonance at 4.614 ppm ($J_{1,2}$ = 8 Hz) shows a H1/H2 cross peak with partial cancellation of the central components indicating equal $J_{1,2}$ and $J_{2,3}$ coupling constants. Although the H2/H3 cross peak is well isolated, its distorted fine structure indicated that the H3 and H4 resonances of this residue are strongly coupled (Widmer & Wuthrich, 1987). These strong coupling effects preclude continued assignment by DQF-COSY, and assignment of proton resonances beyond strong coupling pairs in the residue was obtained from data of the 2D HOHAHA experiment (Figure 1b). A cross section taken through the anomeric proton resonance (4.614 ppm) in the 2D HOHAHA spectrum shows peaks for all the resonances of the spin system including both H6's. Since among

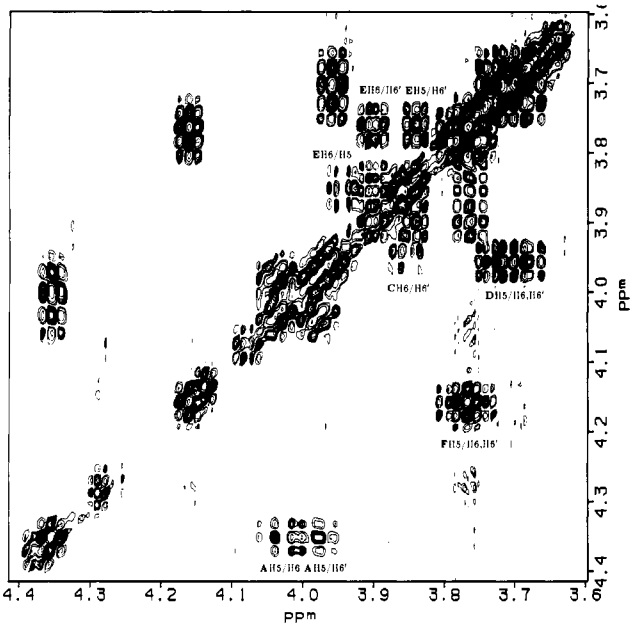

FIGURE 2: Phase-sensitive triple-quantum filtered COSY (TQF-COSY) spectrum of the de-O-acetylated polysaccharide from *S. oralis* ATCC 10557 at 500 MHz. The data matrix was 2 × 256 × 1K complex points with 48 scans per t_1 value. Sine bell apodization with 45° and 90° phase shifts were used in the t_2 and t_1 dimension, respectively. Zero filling in t_1 was used to obtain a 1K × 1K real matrix. Negative contours are drawn dark.

the hexapyranoses present in the polysaccharide this can be possible only for the sugars having the gluco configuration (large vicinal couplings among protons due to trans-diaxial orientation), the identity of the residue was established as β-glucose, residue C.

Assignment of the ^{1}H resonances of the rhamnose residue and the remaining galactose residue was complicated by the small values of $J_{1,2}$. These residues gave anomeric ^{1}H resonances as unresolved ($J_{1,2} \leq 1$ Hz) singlets at 4.888 ppm and at 5.086 ppm with $J_{1,2} \leq 2.5$ Hz. The resonance at 4.888 ppm shows a cross peak to H2 (visible at lower contour level) and connectivity up to the H4 resonance can be traced in the DQF-COSY spectrum. The H3/H4 cross peak shows a distorted fine structure indicating strong coupling between the H4 and H5 resonances. Although connectivity beyond H2 was not seen in the cross section taken through the anomeric resonance in the HOHAHA spectrum, connectivity up to the same H2 resonance was seen in the cross section through the upfield methyl doublet (1.343 ppm) indicating a rhamnosyl residue. Since the anomeric proton signals for both α- and β-anomers of rhamnose have small coupling constants due to the equatorial H2, ^{1}H coupling constant values can not be used to distinguish the anomeric configuration. The anomeric configuration of this residue (**B**) was determined to be β from the 2D NOSEY spectrum (Figure 1c), which shows intraresidue NOE connectivity from H1 to H2, H3, and H5. The anomeric configuration assigned was in good agreement with observed coupling constants ($^1J_{C1H1}$ = 162 Hz) (Bock et al., 1984) as well as with chemical shift values of H5 and H6 (3.46 and 1.343 ppm, respectively) (Jones et al., 1985).

The anomeric resonance at 5.086 ppm ($J_{1,2} < 2.5$ Hz) shows direct correlation to the ^{13}C resonance at 108.56 ppm in the

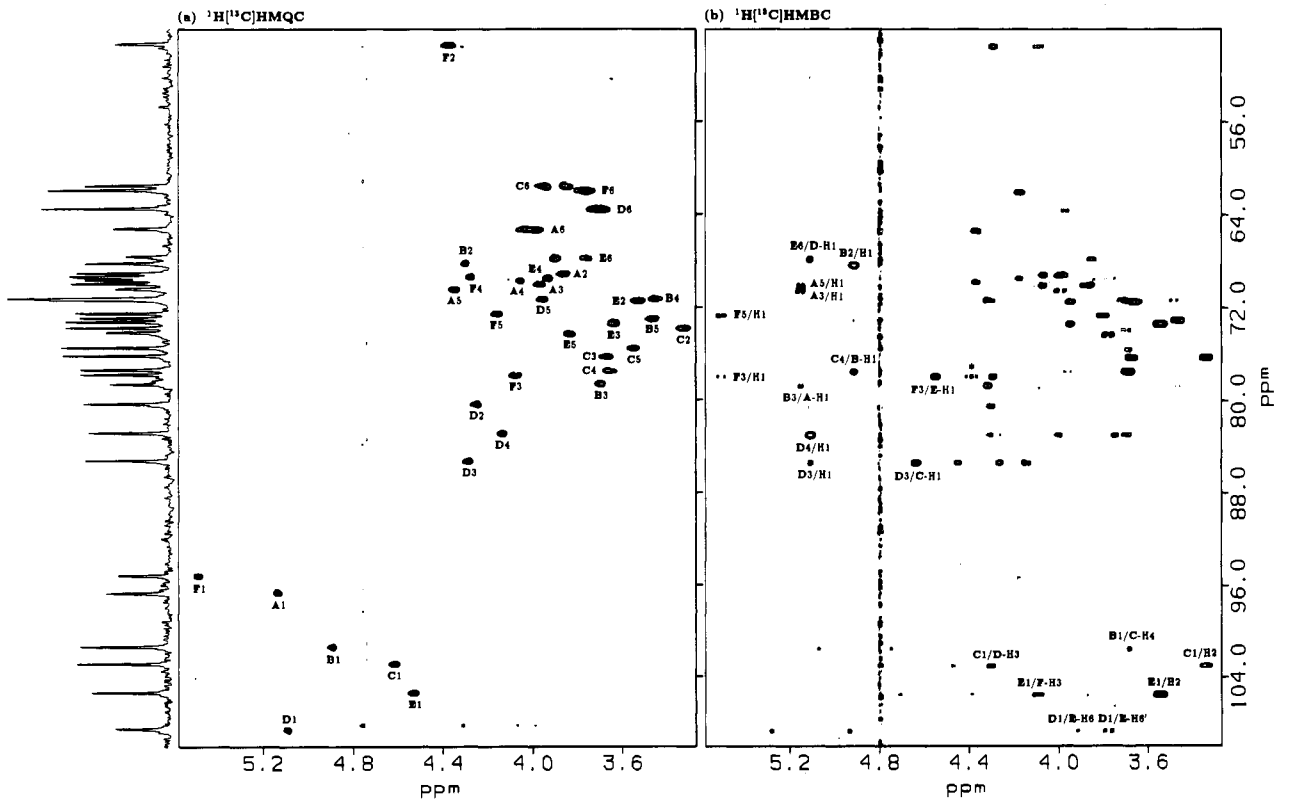

FIGURE 3: (a) Phase-sensitive, ^{13}C-decoupled, ^{1}H-detected multiple-quantum correlation (^{1}H[^{13}C]HMQC) spectrum of the de-O-acetylated polysaccharide from *S. oralis* ATCC 10557 at 500 MHz. The data matrix was 512 × 1K complex points (TPPI) was 32 scans per t_1 value. Sine bell apodization with 45° and 90° phase shifts were used in the t_2 and t_1 dimension, respectively. (b) ^{1}H-detected ^{1}H–^{13}C multiple-bond correlation (^{1}H[^{13}C]HMBC) spectrum at 500 MHz. The data matrix was 2 × 256 × 1K complex points with 48 scans per t_1 value. A 2-Hz Gaussian multiplication was used in the t_2 dimension, and cosine bell apodization was used in the t_1 dimension. The data are presented in mixed mode, absorption in f_1 and absolute value in f_2. Both data matrices were zero filled in t_1 to obtain final data matrices of 1K × 1K (real). The digital resolution is ±0.005 and ±0.1 ppm/pt in the ^{1}H and ^{13}C dimensions, respectively. The normal ^{13}C spectrum of the polymer is displayed at the left hand side. (*) Fold-over peak from GalNAc H2 to the carbonyl carbon of the N-acetyl group.

Table I: NMR Chemical Shifts[a] of the De-O-acetylated and Native[b] Polysaccharide from *S. oralis* ATCC 10557 in D_2O at 25 °C

	residue					
assignment	α-Gal **A**	β-Rha **B**	β-Glc **C**	β-Gal$_f$ **D**	β-Gal **E**	α-GalNAc **F**
^1H						
H1	5.126	4.888	4.614 (+0.054)	5.086 (+0.143)	4.528	5.481
H2	3.854	4.294	3.322 (+0.006)	4.244 (+0.785)	3.525	4.365 (+0.009)
H3	3.962	3.691	3.67	4.280 (+0.151)	3.635	4.070 (+0.017)
H4	4.048	3.45	3.65	4.131 (+0.046)	3.927	4.271 (+0.013)
H5	4.347	3.46	3.545 (−0.029)	3.951 (+0.015)	3.833 (+0.017)	4.154 (+0.200)
H6	4.03	1.343	3.937 (−0.006)	3.72	3.899 (+0.005)	3.770 (+0.520)
H6′	3.98		3.846 (−0.013)	3.68	3.755 (−0.027)	3.750 (+0.520)
NAc						2.045
NH[c]						8.207
OAc					2.141	2.138
^{13}C						
C1	96.67 (171)[e]	101.37 (162)	102.86 (−0.40) (162)	108.56 (−2.26) (175)	105.39 (161)	95.17 (−0.10) (176) [6.0][d]
C2	69.07	68.23	73.80 (−0.06)	80.35 (+2.12)[f]	71.39	49.44 (−0.14) [8.0][d]
C3	69.97	78.66	76.19	85.24 (−2.19)	73.28	77.80 (−0.40)
C4	69.67	71.26	77.40	82.83 (+0.67)	69.42	69.36 (+0.07)
C5	70.42 [8.0][d]	72.96	75.49	71.26 (−0.26)	74.19 (−0.40)	72.54 (−2.51)
C6	65.27 [3.8][d]	17.68	61.57	63.54 (−0.08)	67.65 (−0.60)	61.96 (+2.97)[f]
NAc						
CH_3						22.96
CO						175.56
OAc						
CH_3				22.96		21.12
CO				173.70		174.90

[a] Chemical shifts are with reference to internal acetone (^1H, 2.225 ppm; ^{13}C, 31.07 ppm) and external 85% H_3PO_4 (^{31}P, 0 ppm). [b] Chemical shift values obtained for resonances in O-acetylated repeating units are in parentheses and are reported as deviations from chemical shifts of the de-O-acetylated polymer. [c] These were obtained by the 1331 sequence in H_2O/D_2O at 24 °C. [d] J_{PC} coupling constants were obtained by resolution-enhanced ^{13}C spectra. [e] Anomeric $^1J_{CH}$ (±2.5 Hz) coupling constants are from the HMQC-COSY spectrum of the native polysaccharide. [f] Position of O-acetate substitution.

HMQC spectrum (Figure 3a) indicating that the remaining galactose residue (**D**) is in the β-furanoside form (Beier et al., 1980). All the resonances including H6's were assigned for the Gal$_f$ residue by tracing the cross-peak connectivities in the DQF-COSY spectrum. Wherever possible, proton chemical shift values obtained from the homonuclear correlation spectra for strongly coupled resonances were further refined by the HMQC or HMQC-COSY experiments to be described below.

The triple-quantum filtered COSY (TQF-COSY) spectrum of the de-O-acetylated polysaccharide (Figure 2), which gives cross peaks only for three or more mutually coupled spins, shows cross peaks for all the H5, H6, and H6′ spin systems except one for β-Glc (**C**) residue. The three-spin system for the β-Glc residue showed only a weak cross peak (H6/H6′) in the TQF-COSY spectrum due to small coupling between H5 and one of the H6 resonances (3.937 ppm, $J_{5,6} < 1$ Hz). As expected, no cross peak was detected for the H5 and methyl group of β-rhamnose (Piantini et al., 1982). The sign of the central component of TQF-COSY cross peaks can be used to distinguish between geminal and vicinal protons. All the H6/H6′ cross peaks have positive centers whereas H5/H6 and H5/H6′ cross peaks have negative centers. Since both H6's of β-Glc and H5 of β-Gal$_f$ were assigned previously, TQF-COSY cross peaks involving these resonances can be easily assigned.

Intraresidue NOE connectivities observed in the 2D NOESY spectrum (Figure 1c) can be used to assign H5 resonances of the remaining three residues. β-Gal residue shows NOE cross peaks between H1 and H5 whereas both α-GalNAc and α-Gal residues show H4/H5 connectivity. Assignments obtained by NOE for the α-galactosyl residues were confirmed by HMBC spectra, which show a long-range connectivity between the H1 and C-5 resonances. Therefore, on the basis of these H5 assignments, the remaining H6 and H6′ resonances in the TQF-COSY spectrum can be assigned to individual sugar units. The complete proton assignments for the de-O-acetylated *S. oralis* ATCC 10557 polysaccharide are summarized in Table I.

The 2D NOESY spectrum (Figure 1c) shows several interresidue NOE connectivities (see Table II) in addition to the large number of intraresidue NOE peaks, some of which were discussed above. Even though it is possible to deduce sequence assignments for certains types of linkages from NOE data, no attempt was made here to obtain the linkages of the hexasaccharide from interresidue NOE contacts. The sequence of the hexasaccharide repeating unit was instead obtained from observed long-range ^{13}C–^1H correlations across the glycosidic linkage by the HMBC experiment discussed below.

The ^{13}C spectrum of the de-O-acetylated polymer (see Figure 3) shows six anomeric resonances at 108.56, 105.39, 102,86, 101.37, 96.67, and 95.17 ppm. The spectrum also shows a resonance at 17.68 ppm expected for the methyl carbon of rhamnose and 49.44 ppm together with other characteristic resonances for N-acetamido group (175.56 ppm for the carbonyl carbon and 22.96 ppm for methyl carbon) of residue **F**. The signals at 95.17 and 49.44 ppm show ^{31}P–^{13}C couplings ($^2J_{PC}$ = 6.0 Hz and $^3J_{PC}$ = 8.0 Hz) and were assigned as C-1 and C-2 of α-D-GalNAc-phosphate, residue **F**.

Five methylene carbon resonances at 67.65, 65.27, 63.54, 61.96, and 61.57 ppm are identified by the DEPT experiment. Like polysaccharides from other *Streptococcus* strains 34 and J22 (Abeygunawardana et al., 1989, 1990), the carbon spectrum of this polysaccharide also contains a methylene resonance that shows ^{31}P coupling (65.27 ppm, J_{PC} = 3.8 Hz), suggesting a phosphodiester linkage to C-6 of a hexose.

Table II: Summary of Observed Connectivities in NMR Spectra of *S. oralis* ATCC 10557 De-O-acetylated Polysaccharide[a]

experiment	^{1}H	α-Gal A[b]	β-Rha B	β-Glc C	β-Gal$_f$ D	β-Gal E	α-GalNAc F
HOHAHA	H1	H2, 3, 4	H2	H2, 3, 4, 5, 6, 6′	H2, 3, 4	H2, 3, 4	H2, 3, 4
	H6′		H2, 3, 4, 5				
NOESY	H1	H2	H2, 3, 5	H3, 5	H2, 3	H3, 5	H2
		BH-2[c], 3[c] (w)[d]	CH-4	DH-2[c], 3[c]	EH-6[c], 6′[c]	FH-3	
	H3				H2, 5		H2, 4, 5
	H4	H3, 5					H3, 5
TQF COSY	H6′	H5, 6		H6	H5, 6	H5, 6	H5, 6
^{1}H[^{13}C]HMBC	H1	A3, A5, B3[c] (w)	B2, C4[c]	D3[c]	D3, D4, E6[c]	F3[c]	F3, F5
	H2	A3	B3, B4	C1, C3	D1, D3	E1, E3	F3, NAc[e]
	H3	A2		C2, C4	D2, C1[c]	E2	F2, E1[c]
	H4	A2, A3	B3, B5	C3, C5, B1[c]	D3	E3, E2	F3, F2
	H5	A4, A6	B4		D6	E4, E6	F4, F6
	H6		B4, B5		D4	D1[c]	F5
	H6′				D4	D1,[c] E5	

[a] Except in the case of strong coupling, all protons showed cross peaks in DQF-COSY for vicinal and geminal coupling partners. All protons showed signals arising from one-bond correlations with their attached carbon atoms in the HMQC spectrum. [b] The individual residues are identified by capital letters, and the ^{13}C resonance is indicated by a capital letter and a number for the carbon atom assigned. [c] Interresidue connectivities. [d] (w) weak peak. [e] α-GalNAc H2 shows a long-range connectivity to the carbonyl carbon of the N-acetyl group.

Scheme I

$$[\rightarrow 6)Gal_p(\alpha 1\rightarrow 3)Rha_p(\beta 1\rightarrow 4)Glc_p(\beta 1\rightarrow 3)Gal_f(\beta 1\rightarrow 6)Gal_p(\beta 1\rightarrow 3)GalNAc_p(\alpha 1\rightarrow PO_4^-)]_n$$

A B C D E F

The HMQC spectrum of the de-O-acetylated polysaccharide (Figure 3a) shows resolved correlation peaks for all the ^{13}C–^{1}H single-bond connectivities. All the anomeric and methyl carbon resonances were assigned by correlation to their directly bonded protons. Methylene carbon resonances of residues can be easily assigned by direct correlation to their proton resonances. Once these proton resonances were identified, the remaining protons except strongly coupled spin pairs (β-Rha H4, H5 and β-Glc H3, H4) show chemical shift separation larger than the digital resolution (±0.005 ppm), enabling assignment of all the carbon resonances by direct correlation.

^{13}C assignments for strongly coupled proton resonances were obtained by intraresidue ^{1}H–^{13}C long-range connectivities observed in the HMBC spectrum (Figure 3b). As shown before (Abeygunawardana et al., 1990), the intraresidue long-range correlations observed in the HMBC spectrum depend in a predictable way on the anomeric configuration and the relative stereochemistry of the sugar unit. Correlation peaks are generally observed between resonances for which relatively large two- and three-bond ^{13}C–^{1}H coupling constants have been reported for peracetylated methyl glycosides by Morat et al. (1988).

β-Rha H2 (4.294 ppm) showed long-range correlation to carbon resonances at 78.66 and 71.26 ppm. Since the resonance at 78.66 ppm was already assigned as C-3 of β-Rha, the 71.26 ppm signal was assigned to B4. In the HMQC spectrum, the other ^{13}C resonance (72.96 ppm), which shows a direct cross peak to the H4, H5 strongly coupled pair, was assigned as B5. Once the ^{13}C resonances were identified, accurate chemical shift values for these protons can be obtained from the HMQC spectrum. Similarly, ^{13}C assignments for the strongly coupled pair of β-Glc H3 and H4 were obtained by long-range correlation between H2 and C-3. These ^{13}C assignments together with complete ^{1}H assignments are given in Table I.

In the HMBC spectrum (Figure 3b), all the anomeric protons except H1 of α-GalNAc (residue F) show correlation to the aglycon carbon atom across the glycosidic linkage. It also shows a large number of intraresidue long-range correlations through $^2J_{CH}$ and $^3J_{CH}$ couplings. Relatively few correlations were observed between the aglycone proton and glycosidic carbon resonances. All these connectivities together with connectivities observed in homonuclear experiments are summarized in Table II.

α-Gal (residue A) H1 shows a long-range correlation to C-3, C-5, and β-Rha C-3, indicating Gal(α1→3)Rha linkage in the hexasaccharide. β-Rha H1 shows cross peaks to C-2 and β-Glc C-4, indicating a Rha(β1→4)Glc linkage. Both β-anomeric resonances of Glc (C) and Gal (E) only show correlation across the glycosidic linkages to C-3 of Gal$_f$ and C-3 of α-GalNAc, respectively. The anomeric proton of Gal$_f$ shows connectivity to C-6 of β-Gal in addition to C-3 and C-4 of the same residue. These long-range correlation data show that the hexasaccharide repeating unit of the polysaccharide is as shown in Scheme I.

The position of the phosphodiester linkage is suggested by the ^{31}P scalar couplings observed in the ^{1}H and ^{13}C spectra. Since both C-6 and C-5 of the α-Gal residue show ^{13}C–^{31}P couplings, the phosphodiester linkage was assigned to C-6 of residue A.

Native Polysaccharide. Knowledge of the structure of the de-O-acetylated polymer greatly facilitates the interpretation of the NMR spectrum of the native polymer, which, on account of the partial acetylation, is extremely complicated. The ^{1}H NMR spectrum of the native polysaccharide at 600 MHz showed three resonances at 5.229 ($J < 1$ Hz), 5.029 ($J < 2$ Hz), and 4.668 ($J = 7.8$ Hz) ppm in the anomeric region in addition to those assigned for the de-O-acetylated polymer. The anomeric resonances of β-Gal$_f$ and β-Glc showed reduced intensities, while the anomeric resonances of β-Rha, β-Gal, α-Gal, and α-GalNAc retained the same intensities as in the de-O-acetylated polymer. The resonances unique to the native polymer were approximately $^1/_3$ the intensity of the anomeric resonances whose intensities were unchanged from those of the de-O-acetylated polymer.

Substitution of a sugar residue by O-acetyl groups changes the chemical shifts of both ^{1}H and ^{13}C resonances at the position of substitution, at other positions on the same sugar residue, and at positions of adjacent residues in the polysaccharide (Bundle et al., 1986). Empirical chemical shift rules have been used to assign positions of O-acetate substitution of polysaccharides. A large downfield shift (0.8–0.5

ppm) for the resonance of the proton bonded to the carbon to which the O-Ac is attached most often coincides with a downfield shift of the carbon atom resonance (1.5–4.0 ppm) and an upfield shift of the signals assigned to adjacent carbon atoms (Bock & Pederson, 1983). The ^{1}H NMR spectrum of the native polysaccharide indicated two distinct positions of O-acetate substitution with each occupying $^1/_3$ of the repeating units.

In addition to spectral lines arising from partial acetylation, the interpretation of the spectrum of the native polymer was further complicated by spontaneous depolymerization caused by hydrolysis of the phosphodiester linkage in the polymer backbone. Since complications in the spectra render difficult the precise assignment of the positions of O-acetylation by chemical shift methods, a method based on long-range ^{13}C–^{1}H coupling was used in this work (Dabrowski et al., 1987). Therefore it is necessary to assign all the ^{1}H and ^{13}C resonances in the native polysaccharide.

Most of the proton assignments can be obtained by the homonuclear 2D experiments discussed earlier for the de-O-acetylated polymer. Due to the complexity of the ^{13}C spectrum, heteronuclear correlation experiments such as HMQC and HMBC were supplemented by the combination technique HMQC-COSY. Iterative comparison of spectra from these three experiments yielded complete ^{1}H and ^{13}C assignments for the native polysaccharide. Finally, O-acetate substituents were located by long-range correlation from protons on α-carbon atoms to carbonyl carbon resonances of O-acetate groups by using HMBC spectra.

In the ^{1}H homonuclear 2D spectra, some of the cross peaks arising from coupled protons showed complicated patterns not observed in spectra of the de-O-acetylated polymer due to the overlap of cross peaks from sugar residues in acetylated and unsubstituted repeating units. The spin system starting with the anomeric resonance of α-GalNAc phosphate residue (**F**), for example, showed composite cross peaks in the DQF-COSY spectrum. Although contributions from unsubstituted and acetylated repeating units carry different intensities, accurate chemical shifts of these overlapping resonances could not be obtained in homonuclear 2D spectra. Since most of the resonances of the carbon atoms connected to these overlapping ^{1}H resonances show greater shift dispersion in the ^{13}C dimension, accurate proton chemical shifts were determined from the heteronuclear spectra.

In the following discussion, residues in the unsubstituted repeating units will be identified by a capital letter (see Scheme I) and residues in the O-acetylated repeating units will be identified by a letter followed by prime (e.g., **C′**) with no attempt made to distinguish particular O-Ac substitution positions.

The resonance at 5.229 ppm ($J < 1$ Hz) shows a weak cross peak in the DQF-COSY spectrum to the H2 resonance at 5.029 ppm, and in the HOHAHA spectrum it shows weak cross peaks to resonances at 5.209 and 4.431 ppm. In the HMQC spectrum, resonances at 5.229 and 5.029 ppm show directly bonded ^{13}C resonances at 106.37 and 82.51 ppm indicating that the latter belongs to a nonanomeric proton. The assignments can be extended in the DQF-COSY spectrum to obtain the rest of the resonances in the spin system from H2. The fine structure of H2/H3, H3/H4, and H4/H5 cross peaks were identified as those of the β-Gal$_f$ residue, which had its anomeric signal at 5.086 ppm with $^2/_3$ of the intensity of unaffected signals. These data indicated that the spin system belongs to the β-Gal$_f$ residue (**D′**) of O-acetylated repeating units in the polymer. The H2 resonance had a large downfield shift ($\Delta = 0.785$ ppm) together with a downfield shift of the C-2 atom ($\Delta = 2.12$ ppm) and upfield shifts of C-1 ($\Delta = 2.26$ ppm) and C-3 ($\Delta = 2.19$ ppm) atoms compared to values obtained for the de-O-acetylated polymer, indicating that one of the O-acetate groups is linked to C-2 of β-Gal$_f$. This tentative assignment of the position of O-acetylation was confirmed by HMBC experiments as will be described below. A troublesome complication in the identification of this residue came from the overlapping α-anomeric signal of the reducing terminal GalNAc residue (5.225 ppm, $J = 3.6$ Hz) arising from autohydrolysis of the phosphodiester linkage of the polymer backbone.

A small signal at 5.138 ppm ($J = 3.6$ Hz) that overlaps with the ^{1}H resonance at 5.126 ppm ($J = 3.6$ Hz) assigned as H1 of α-Gal-6-phosphate (phosphodiester) in the de-O-acetylated polymer was identified as H1 of α-Gal-6-phosphate (phosphomonoester) resulting from partial hydrolysis of the polymer. The DQF-COSY spectrum shows overlapping cross peaks with identical chemical shifts for both H2 resonances. H3/H4 cross peaks in the DQF-COSY spectrum and cross sections taken through anomeric protons in the HOHAHA spectra show overlapping H3 and resolved H4 resonances in these residues. All these resonances are assigned to residue **A** and O-acetylation of the repeating subunit has no measurable influence on the chemical shifts of this residue.

The ^{1}H signals of residues β-Gal$_f$ (**D**), β-Rha (**B**), β-Glc (**C**), and β-Gal (**E**) were assigned from their respective anomeric protons (5.086, 4.888, 4.614, and 4.528 ppm) as described previously for de-O-acetylated polymer. These assignments show no detectable chemical shift differences when compared to those obtained for de-O-acetylated polymer. However, a HOHAHA cross section taken through β-Gal H1 shows broadening of the H4 cross peak indicating possible chemical shift changes in resonances H4 and beyond (H5, H6, H6′) for β-Gal residues in O-acetylated subunits. The remaining anomeric resonance at 4.668 ppm was identified as H1 of β-Glc from DQF-COSY and HOHAHA spectra. Since it accounts for the reduced intensity of β-Glc H1 resonance at 4.614 ppm, this residue was assigned as β-Glc (**C′**) in O-acetylated subunits in the polysaccharide. These ^{1}H chemical shift changes due to O-acetate substituted at Gal$_f$ C-2 can be best seen in the 2D NOESY spectrum (Figure 4).

The TQF-COSY spectrum (Figure 5) of the native polymer shows complicated cross peaks for β-Gal, β-Gal$_f$, and β-Glc residues. Extensive overlapping of cross peaks for these residues suggests slightly different chemical shifts of H5 and H6 resonances in O-acetylated and unsubstituted repeating units. The three-spin system assigned to the α-Gal residue **A** also gave overlapping cross peaks for H5/H6 and H5/H6′ in the spectrum. But unlike the other three residues, these additional resonances are assigned to α-Gal-6-phosphate (phosphomonoester) resulting from autohydrolysis of the polymer rather than O-acylation. Cross peaks with multiplicity and chemical shift values identical with those assigned to α-GalNAc H5 and H6 in the TQF-COSY spectrum of the de-O-acetylated polymer appear in Figure 5, and a new set of cross peaks appears at 4.35/4.29 ppm of the spectrum. Although severe overlapping of the cross peaks and diagonal peaks precluded assignments of these signals from the TQF-COSY spectrum, accurate chemical shift values for all H5, H6, and H6′ resonances were obtained from heteronuclear correlation spectra and 2D NOESY spectrum discussed below.

Most of the ^{13}C assignments of the native polymer were obtained by HMQC (Figure 6) and HMBC (Figure 7) spectra as described above for the de-O-acetylated polymer. The

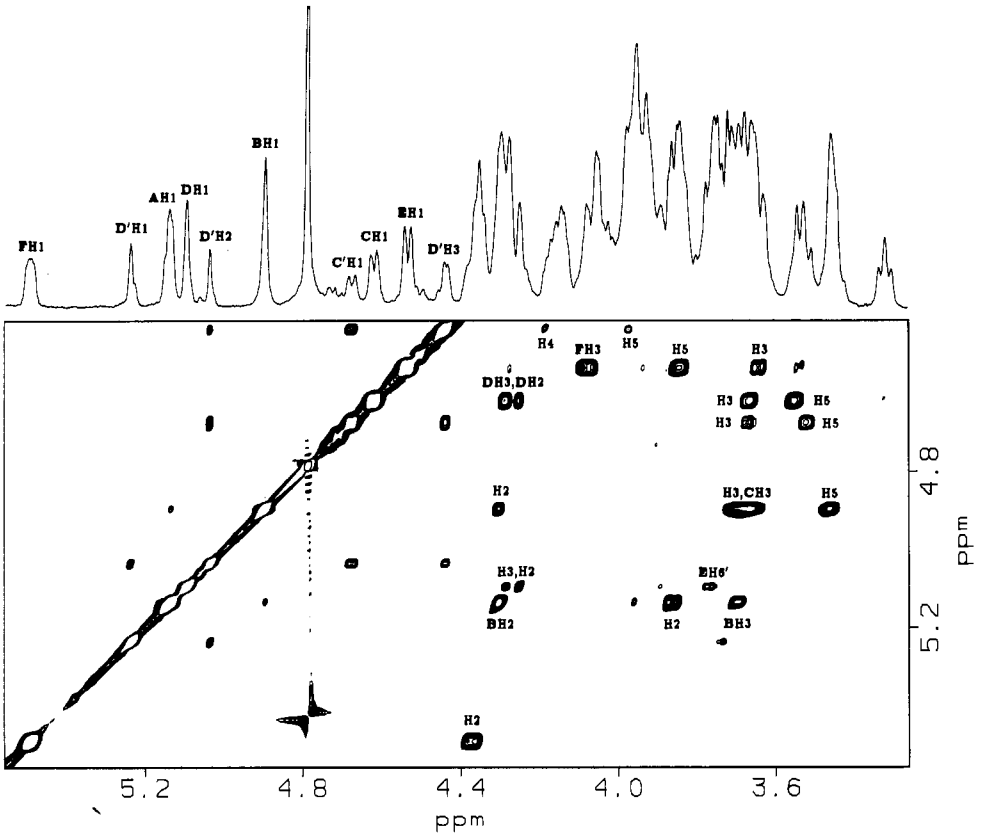

FIGURE 4: 2D NOESY spectrum of the native polysaccharide from *S. oralis* ATCC 10557 at 500 MHz. The data matrix was 2 × 256 × 1K complex points with 8 scans per t_1 value and a 350-ms mixing time. Gaussian line broadening (3.0 Hz) in the t_2 dimension and shifted sine bell (65°) in the t_1 dimension were used prior to Fourier transformation. All spectra were zero filled in the t_1 dimension to obtain 1K × 1K (real) matrices with a digital resolution of ±0.005 ppm/pt. Part of the 1D spectrum is displayed at the top.

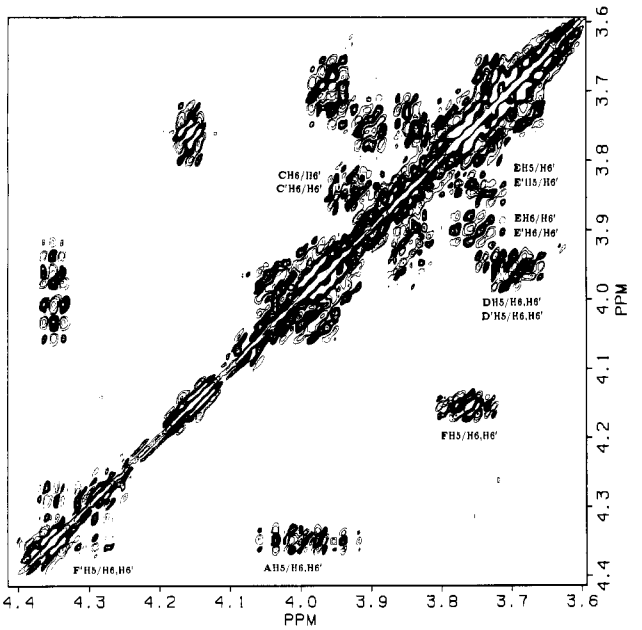

FIGURE 5: Phase-sensitive triple-quantum filtered COSY (TQF-COSY) spectrum of the native polysaccharide from *S. oralis* ATCC 10557 at 500 MHz. The data matrix was 2 × 128 × 512 complex points with 120 scans per t_1 value. A spectral width of ±600 Hz was used with the upfield methyl signals folded into the spectrum. Sine bell apodization with 20° and 45° phase shifts were used in the t_2 and t_1 dimension, respectively. Zero filling in both dimensions were done to obtain a 1K × 1K (real) matrix. Negative contours are drawn dark.

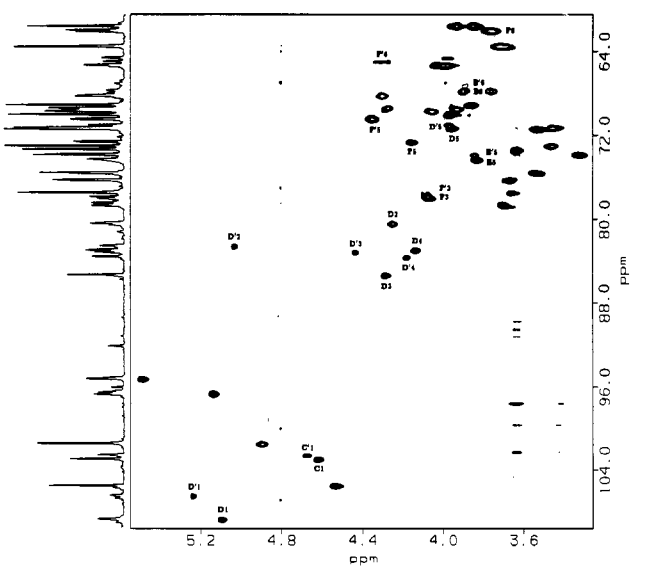

FIGURE 6: Phase-sensitive, ^{13}C-decoupled, ^1H-detected multiple-quantum correlation ($^1H[^{13}C]$HMQC) spectrum of the native polysaccharide from *S. oralis* ATCC 10557 at 500 MHz. The data matrix was 512 × 1K complex points (TPPI) with 32 scans per t_1 value. Processing parameters were 2-Hz Gaussian multiplication in t_2 and cosine bell apodization and zero filling in the t_1 dimension to obtain 1K × 1K (real) matrices. The normal ^{13}C spectrum of the polymer is displayed at left hand side. Only the peaks that are relevant to locate O-acetate substituents are labeled in the figure.

HMQC spectrum of the native polysaccharide shows isolated correlation peaks for the β-Gal$_f$ residue (**D'**), which was O-acetylated at the C-2 position. D5 and D'5 cross peaks were slightly overlapping whereas D6 and D'6 gave unresolved correlation peaks. Residues **A** (α-Gal) and **B** (β-Rha) did not show any change in chemical shift values (both ^1H and ^{13}C) in O-acetylated subunits compared to the unsubstituted sub-

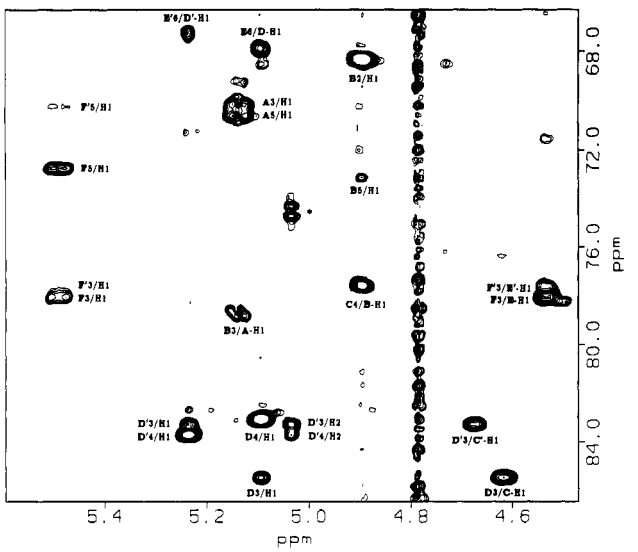

FIGURE 7: Expanded region of (^{1}H[^{13}C]HMBC) spectrum of the native polysaccharide at 500 MHz. The data matrix was 2 × 256 × 1K complex points with 128 scans per t_1 value. Processing parameters are identical with those of the HMQC spectrum (Figure 6), and the data are presented in mixed mode, absorption in f_1 and absolute value in f_2. (*) Fold-over peak to carbonyl carbon of O-acetate group.

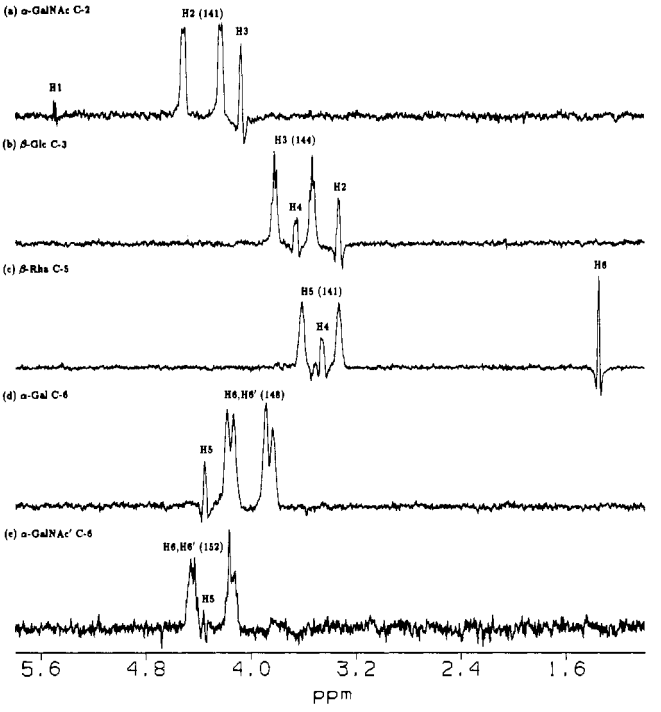

FIGURE 8: Cross sections of the two-dimensional HMQC-COSY spectrum of the native polysaccharide from *S. oralis* ATCC 10557. The data matrix was 2 × 256 × 1K complex points with 112 scans per t_1 value. A 4-Hz exponential line broadening in t_2 and a cosine bell apodization in t_1 were used prior to Fourier transformation. Data were zero filled in t_1 to obtain 1K × 1K real matrix. Cross sections taken through carbon frequencies (a) GalNAc C-2 at 49.43 ppm, (b) β-Glc C-3 at 76.17 ppm, (c) β-Rha C-5 at 72.94 ppm, (d) α-Gal C-6 at 65.27 ppm, and (e) α-GalNAc′ C-6 at 64.93 ppm. One-bond ^{1}H–^{13}C coupling constants (±2.5 Hz) are in parentheses.

units. Even though most of the ^{1}H resonances of β-Glc in the O-acetylted subunits (**C′**) had different chemical shifts, only the C′-1 resonance shows any detectable difference in the ^{13}C dimension. The H5 and H6 resonances of residue **E′** gave slightly overlapping correlation peaks with E5 and E6 peaks. Due to better separation of these resonances in the ^{13}C dimension ($\Delta > 0.4$ ppm), accurate ^{1}H and ^{13}C assignments can be easily obtained from the HMQC spectrum. The rest of the resonances of residue **E′** did not show any detectable difference from residue **E**.

However, when correlation peaks from unsubstituted and O-acetylated repeating units overlap, HMQC was not a preferred technique to extract chemical shifts. The greater line widths of ^{13}C bound protons together with the low digital resolution in the ^{13}C dimension in HMQC spectra makes overlapping peaks indistinguishable. In the HMQC spectrum (Figure 6), the F1, F2, F3, and F4 correlation peaks for residues **F** overlap with respective peaks from **F′**. Accurate chemical shifts for resonances involved in these peaks were obtained from an HMQC-COSY method recorded without ^{13}C decoupling during the acquisition, which provides a powerful method for supplementing HMQC and HMBC data. In this experiment a cross section taken through a particular carbon frequency shows direct correlation peaks (split by $^1J_{CH}$ couplings), which are analogous to diagonal peaks in the COSY spectrum, and relay peaks to vicinal proton resonances. Large vicinal proton couplings give stronger relay peaks whereas smaller couplings tend to give weaker peaks. This is illustrated in Figure 8a, which shows a cross section taken through the resonance of C-2 of the α-GalNAc residue **F**, which shows an intense cross peak to the resonance of H3 and a weaker cross peak to that of H1. This is also a straightforward method for assigning strongly coupled vicinal protons, which are quite common in carbohydrate NMR spectra. Since direct peaks are split by larger one-bond couplings, relay peaks that appear in the middle of split direct peaks can be accurately assigned. Figure 8b,c, showing cross sections taken through C-3 of β-Glc and C-5 of β-Rha residues, provides assignments for the strongly coupled pairs of β-Glc H3 and H4 and β-Rha H4 and H5.

This method was utilized in the assignment of a particularly difficult yet important group of peaks in the HMQC spectra at 64.96 and 64.63 ppm in the ^{13}C dimension. ^{1}H chemical shifts suggested that the latter signal should be assigned to the C-6 resonance of α-Gal-6-phosphate (phosphomonoester) resulting from autohydrolysis of the polymer. Since the other ^{13}C resonance shows a broad correlation peak with unresolved ^{1}H resonances (4.29 ppm) in agreement with the unassigned cross peak observed in the TQF-COSY (Figure 5), it was identified as methylene carbon. However, this cross peak had a positive center indicating either well-separated H6 resonances or resolved H5 and strongly coupled H6 resonances. Since H5 of the spin system was not assigned, this led to ambiguities in the assignment and identification of the spin system that were resolved by the following considerations.

In the HMBC spectrum (Figure 7) the α-GalNAc H-1 resonance shows a weak long-range correlation peak to the ^{13}C resonance at 70.03 and 77.4 ppm in addition to resonances assigned to the unsubstituted **F** residue C-5 and C-3 (72.54 and 77.80 ppm). Since the C-3 resonance at 77.4 ppm agrees with the F′3 cross peak in the HMQC spectrum, the other ^{13}C resonance was identified as C-5 of the **F′** residue. However, the ^{1}H chemical shift of H-5 for **F′** could not be obtained by HMQC due to overlapping F′5 and A5 cross peaks in the HMQC spectrum. Accurate chemical shifts of H5 of the **F′** residue and most of the other overlapping resonances can be easily obtained by the coupled HMQC-COSY experiment. Figure 8d,e shows cross sections taken through the A6 and F′6 carbon resonances. These cross sections provided accurate ^{1}H assignments for the respective H5 resonances. With accurate chemical shifts for H5, it became apparent that the unusual TQF-COSY cross peak for **F′** residue was due to

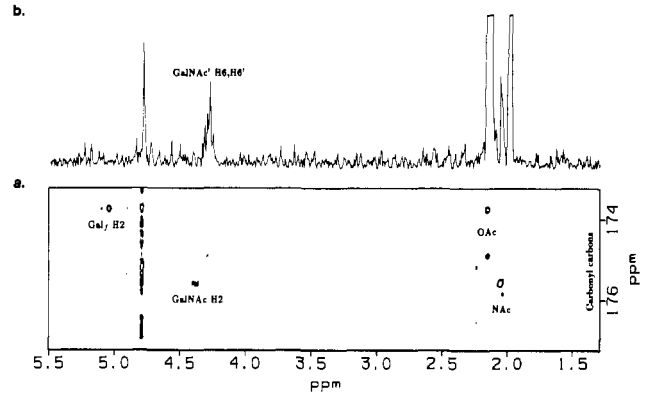

FIGURE 9: (a) ^{1}H-detected ^{1}H–^{13}C multiple-bond correlation (HMBC) spectrum of the native polysaccharide from *S. oralis* ATCC 10557. Spectra were recorded with low-power ^{13}C pulses (90° ^{13}C ≈ 285 μs) selecting the carbonyl carbon region of the ^{13}C spectrum. The data set was 2 × 30 × 1K complex points with 512 scans per t_1 value. Matched apodization in t_2, cosine bell function in t_1, and zero filling were done to obtain a 256 × 1K real spectrum. For clarity contours arising from intense correlation peaks from methyl protons are plotted at 10 times higher level than the rest of the spectrum. (b) Cross section taken through the O-acetyl carbonyl carbon at 174.9 ppm.

strongly coupled H6 protons centered at 4.29 ppm. These chemical shift values observed for the native polysaccharide are tabulated in Table I as differences from values observed for the de-O-acetylated polysaccharide.

Given the complete assignment of the ^{13}C and ^{1}H chemical shifts of the sugar ring atoms of both the acetylated and unsubstituted subunits of the native polysaccharide, rigorous assignment of the positions of partial acetylation was possible with a variation of the HMBC experiment. The use of low-power ^{13}C pulses selecting the carbonyl carbon region of the spectrum allows a narrow sweep width in the ^{13}C dimension with a small number of t_1 values greatly improving the efficiency of data acquisition. In this experiment (Figure 9) H2 of the **D′** residue shows a long-range correlation to the signal of the carbonyl carbon of an O-acetate group at 173.70 ppm confirming one O-acetate linkage to the Gal$_f$ C-2 carbon. α-GalNAc H2 shows a correlation to the carbonyl carbon of the N-acetyl group. Although not visible at the contour level shown in Figure 9a, cross sections (Figure 9b) taken through the other O-acetyl carbonyl carbon (174.9 ppm) show a long-range correlation to proton resonances centered at 4.29 ppm, which were assigned as H6 protons of **F′**. The assignment of the positions of partial acetylation to C-2 of β-Gal$_f$ (**D′**) and to C-6 of α-GalNAc (**F′**) is consistent with the acetylation shifts summarized in Table I.

At the resolution of the two-dimensional spectra (±0.005 ppm), chemical shift changes due to the O-acetate group at C-2 of Gal$_f$ can be detected for resonances assigned to the β-Glc, β-Gal$_f$, and β-Gal residues, whereas shift changes due to the O-acetate group at C-6 of the α-GalNAc residue can be detected only within the residue. However, strong resolution enhancement of a one-dimensional proton spectrum recorded at 600 MHz shows that O-acetate substitution at F′6 causes a downfield shift ($\Delta\delta$ = 0.005 ppm) of the anomeric ^{1}H resonance of β-Glc resulting in splitting of β-Glc H1 at 4.614 ppm (residue **D**) into two signals with equal intensity. The anomeric proton resonance of β-Glc at 4.668 ppm (residue **D′**) showed a set of signals appearing downfield ($\Delta\delta$ = 0.006 ppm) with very low intensity indicating a low abundance of repeating units with O-acetate groups at both positions. These data, together with NMR studies of fragments isolated from autohydrolysis of the polysaccharide, suggest that the *S. oralis* ATCC 10557 polysaccharide is randomly O-acetylated in the repeating units (Abeygunawardana and Bush, in preparation).

On the basis of these reuslts, we propose the following structure for the polysaccharide in *S. oralis* ATCC 10557:

$$[\rightarrow 6)\text{Gal}_p(\alpha 1\rightarrow 3)\text{Rha}_p(\beta 1\rightarrow 4)\text{Glc}_p(\beta 1\rightarrow 3)\text{-}$$

$$\text{Gal}_f(\beta 1\rightarrow 6)\text{Gal}_p(\beta 1\rightarrow 3)\text{Gal}_p\text{NAc}(\alpha 1\rightarrow \text{PO}_4^-\text{-}]_n$$

$$\begin{matrix} 2 & & 6 \\ \uparrow & & \uparrow \\ (\text{OAc})_{0.33} & & (\text{OAc})_{0.33} \end{matrix}$$

In the course of our discussion of the chemical shift changes resulting from the presence of O-acetate substituents in the polysaccharide from *S. oralis* ATCC 10557 and the assignment of its structure, we have referred to a varying degree of depolymerization observed in the different 2D NMR spectra indicating that the polysaccharide is unstable in D_2O solution at room temperature. Hydrolysis of the glycosyl phosphate linkage of the α-GalNAc residue (**F**) introduces additional resonances in the anomeric region at 5.220 and 4.700 ppm for reducing terminal GalNAc α- and β-anomeric resonances and two sets of β-Gal (residue **E**) anomeric resonances at 4.497 and 4.443 ppm. The extent of the depolymerization can be easily monitored by the intensity of the anomeric proton resonance of α-GalNAc phosphate at 5.482 ppm. Prolonged standing of the sample in D_2O solution results in reduction of intensity of the resonance at 5.482 ppm by $^1/_3$ and the disappearance of signals assigned to F′6 O-acetyl group (2.138 ppm). The NMR spectrum also shows a new resonance at 2.084 ppm which is identical with the methyl resonance of free acetic acid in D_2O at the same pH (pD 3.0). Some hydrolysis has been observed for the polysaccharide sample used for the NMR studies in H_2O/D_2O solution at low pH (≈2). After lyophilization and redissolving in D_2O, this sample showed partial depolymerization, which on heating at 65 °C for 1 h gave reduced ($^1/_3$) intensity of the α-GalNAc phosphate H1 resonance. Heating the sample at 80 °C for 3 h did not increase the depolymerization yield, indicating that the cleavage of F′6 O-acetate group is correlated with cleavage of the glycosyl phosphate linkage. This interpretation was supported by the fact that no depolymerization was observed for the de-O-acetylated polymer even at higher temperature.

Discussion

Covalent structure determination of complex carbohydrates by multinuclear NMR methods utilizing through-bond correlations offers substantial advantages over chemical methods as well as methods based on interpretation of NMR data by chemical shift analogies. Here we demonstrate successful application of different 2D NMR methods to obtain the primary structure of a polysaccharide with substantial complexity. Once the sugar composition of the polysaccharide is known, ^{1}H NMR coupling constant data can be correlated with analytical data to unambiguously identify each sugar residue in the repeating unit. Complete ^{1}H and ^{13}C resonance assignments and linkage assignments by ^{1}H–^{13}C long-range correlation enable determination of the covalent structure of the repeating unit. ^{31}P coupling to ^{1}H and ^{13}C resonances are utilized to obtain phosphate linkage positions in the polymer.

Determination of the complete structure of a polysaccharide with labile side chains such as pyruvate or O-acetate by classical chemical methods can be quite difficult. Almost any chemical treatment capable of cleaving glycosidic linkages is likely to disturb the side chains, thus preventing their detection. In such cases, spectroscopic methods not requiring any chemical steps prior to recording the initial data can be valuable. In the method described here, NMR spectra recorded directly

on a native polysaccharide preparation reveal the presence of the side chains. Although the complexity of these spectra prevents a direct structural interpretation, the labile side chains can then be readily removed leading to a simple structure amenable to solution by 2D NMR methods. Once the backbone structure of the polysaccharide is assigned, interpretation of the more complicated spectrum of the native polysaccharide can provide the exact positions of the substituents.

A series of rules for changes in ^{13}C and ^{1}H chemical shifts resulting from acetylation of carbohydrates has been proposed for assignment of positions of O-acetylation in polysaccharides. Like all empirical chemical shift correlations, these rules are not rigorous, and their application can lead to errors or ambiguities especially in cases of multiple positions of acetylation or acetylation in adjacent positions. Since the carbonyl-selective HMBC method used in this work depends on three-bond coupling correlation, it does not suffer this disadvantage. Carbonyl ^{13}C resonances show large cross peaks in HMBC to the sharp singlet methyl proton resonances of acetates due to the substantial geminal coupling constant of 6.9 Hz (Uhrinova et al., 1990). Assignment of the positions of acetylation is deduced from the smaller cross peaks to the previously assigned signals of the sugar ring protons. The cross peak used for assignment of the acetylation at C-6 residue F′ (Figure 9b) is especially small due in part to the fact that the vicinal coupling for methylene protons (3.0 Hz) is smaller than that for methine proton (3.7 Hz) (Uhrinova et al., 1990) and partly due to the broad and complex structure of the H6, H6′ multiplet resulting from large homonuclear coupling constants.

Our NMR results show that the receptor polysaccharide of *S. oralis* 10557 is closely related to those of *S. oralis* 34 and *S. mitis* J22 as well as to certain capsular polysaccharides of *Streptococcus pneumoniae*, most notably type 20 (Richards et al., 1983). Each polysaccharide is composed of repeating hexa- or heptasaccharide units that are linked by phosphodiester bonds. Whereas the capsular polysaccharides of pneumococci have generally been isolated from growth media, those of the *S. oralis* and *S. mitis* strains appear to be firmly attached to the bacterial cell wall where they served as receptors for the lectins of *A. viscosus* and *A. naeslundii* as well as for certain other galactose and *N*-acetylgalactosamine reactive bacterial lectins (Cisar, 1986). Different lectin specificities have been detected on bacteria such as *Capnocytophage ochracea* ATCC 33596, an organism that participates in a L-rhamnose inhibitable coaggregation with *S. sanguis* H1 (Cassels & London, 1989). The structure of a hexasaccharide isolated from the H1 polysaccharide has been determined by a combination of methods including NMR (Cassels et al., 1990). Further studies with the native H1 polysaccharide will enable the structural comparison of this molecule with those of strains 10557, 34, and J22.

The specificity of lectin-mediated adherence of certain *A. viscosus* and *A. naeslundii* strains has been examined by a number of different approaches. The most potent inhibitors of the coaggregations of these bacteria with *S. oralis* 34 were structures containing Gal(β1→3)GalNAc (McIntire et al., 1983), while GalNAc(β1→3)Galα-OMe was somewhat less active (McIntire et al., 1988). Similarly, studies of bacterial attachment to asialofetuin-coated latex beads identified the Gal(β1→3)GalNAc termini of O-linked oligosaccharide chains as receptors and using this model system established the recognition of terminal galactose by the *Actinomyces* lectin from the effect of galactose oxidase on the glycoprotein (Heeb et al., 1982). Results of bacterial binding to glycolipids on thin-layer chromatograms also identified a number of structures with terminal Gal(β1→3)GalNAcβ- or GalNAc(β1→3)Galα as receptors for the *A. naeslundii* WVU45 (ATCC 12104) lectin (Brennan et al., 1987; Strömberg & Karlsson, 1990). Strömberg and Karlsson (1990) have interpreted these results to indicate binding of terminal or internal GalNAcβ but not Galβ by the *A. naeslundii* lectin and suggested a specificity that involves recognition of the β-linkage, the acetamido group, and the axial hydroxyl at C-4 of GalNAc by a small lectin combining site. This interpretation fails to account for the generally similar inhibition of lectin-mediated bacterial adherence by both galactose and *N*-acetylgalactosamine (McIntire et al., 1983) and also the activities of the receptor polysaccharides of strains 10557 and J22, each of which lack of GalNAcβ. These results are consistent with the binding of *Actinomyces spp.* lectins to the Gal(β1→3)GalNAc as well as GalNAc(β1→3)Gal termini of glycolipids (Brennan et al., 1987), a possibility that implies maximum complimentarity for certain common features of these disaccharides (Cisar et al., 1989). Some contribution of the 2-acetamido group to lectin recognition is also possible since the lectin-mediated coaggregation of *A. naeslundii* with *S. oralis* 34 was inhibited more effectively by *N*-acetylgalactosamine than by galactose while the reverse was true for the coaggregation of *A. viscosus* T14V (McIntire et al., 1983). In addition, lectin-mediated bacterial attachment to other structures such as as the Gal(β1→4)GlcNAc termini of asialo-α_1-acid glycoprotein has also been observed under conditions that favored a relatively high receptor density (Heeb et al., 1982).

A comparison of the cell wall polysaccharide of *S. oralis* 10557 with those of *S. oralis* 34 and *S. mitis* J22 shows that each different repeating unit contains an internal galactofuranose linked (β1→6) to Gal(β1→3)GalNAcα or GalNAc(β1→3)Galα. These internal disaccharide structures represent potential sites of lectin recognition that may be exposed by the flexible (β1→6) linkage from Gal$_f$. If so, partial O-acetylation at the 6-OH of GalNAc in the 10557 polysaccharide may not affect lectin binding since branching at this position did not diminish the receptor activities of certain other Gal(β1→3)GalNAc-containing structures (McIntire et al., 1983; Strömberg & Karlsson, 1990). However, partial O-acetylation at the 6-OH of GalNAc was correlated with spontaneous depolymerization of the native 10557 polysaccharide under mild conditions at room temperature, presumably by an effect of this substitution on the lability of the adjacent glycosyl phosphate bond. The biological significance of this reaction is unknown as are the effects of partial O-acetylation at the 2-OH of Gal$_f$ in the polysaccharide. Previous studies have shown that serological specificity of the *S. oralis* 34 polysaccharide involves the α-GalNAc end of the hexasaccharide subunit (McIntire et al., 1988). By analogy, antigenicity of the J22 and 10577 polysaccharides may involve the rhamnose branch of the former and the Gal(α1→3) as well as Glc(β1→3) of the latter. Results from previous studies of the 10557 polysaccharide suggested that GalNAc was an immunodeterminant (Koga et al., 1983); however, this proposal was based on the inhibition of immunoprecipitation by a very high concentration of the monosaccharide. Further studies with oligosaccharide fragments of these polysaccharides are in progress to firmly establish their respective antigenic and receptor regions.

ACKNOWLEDGMENTS

We thank the National Magnetic Resonance Facility at Madison, supported by NIH Grant RR-02301, for Bruker NMR data and Dr. Ann Sandberg for critically reading the

manuscript. We acknowledge the help of Liqiang Xu for the carbohydrate analysis.

REFERENCES

Abeygunawardana, C., Bush, C. A., Tjoa, S. S., Fennessey, P. V., & McNeil, M. R. (1989) *Carbohydr. Res. 191*, 279–293.

Abeygunawardana, C., Bush, C. A., & Cisar, J. O. (1990) *Biochemistry 29*, 234–248.

Bax, A., & Davis, D. G. (1985) *J. Magn. Reson. 65*, 355–360.

Bax, A., & Summers, M. F. (1986) *J. Am. Chem. Soc. 108*, 2093–2094.

Bax, A., & Marion, D. (1988) *J. Magn. Reson. 78*, 186–191.

Bax, A., Griffey, R. H., & Howkins, B. L. (1983) *J. Magn. Reson. 55*, 301–315.

Beier, C. R., Mundy, B. P., & Strobel, G. A. (1980) *Can. J. Chem. 58*, 2800–2804.

Bock, K., & Pedersen, C. (1983) *Adv. Carbohydr. Chem. Biochem. 41*, 27–66.

Bock, K., Pedersen, C., & Pedersen, H. (1984) *Adv. Carbohydr. Chem. Biochem. 42*, 193–225.

Braunschweiler, L., & Ernst, R. R. (1983) *J. Magn. Reson. 53*, 521–528.

Brennan, M. J., Cisar, J. O., & Sandberg, A. L. (1986) *Infect. Immun. 52*, 840–845.

Brennan, M. J., Joralmon, R. A., Cisar, J. O., & Sandberg, A. L. (1987) *Infect. Immun. 55*, 487–489.

Bundle, D. R., Gerken, M., & Perry, M. B. (1986) *Can. J. Chem. 64*, 255–264.

Cassels, F. J., & London, J. (1989) *J. Bacteriol. 171*, 4019–4025.

Cassels, F. J., Fales, H. M., London, J., Carlson, R. W., & Van Halbeek, H. (1990) *J. Biol. Chem. 265*, 14127–14135.

Cisar, J. O. (1986) in *Microbial Lectins and Agglutinins: Properties and Biological Activity* (Mirelman, D., Ed.) pp 183–196, John Wiley and Sons, New York.

Cisar, J. O., Brennan, M. J., & Sandberg, A. L. (1985) in *Molecular Basis of Oral Microbial Adhesion* (Mergenhagen, S. E., & Rosan, B., Eds.) pp 159–163, American Society for Microbiology, Washington, DC.

Cisar, J. O., Brennan, M. J., & Sandberg, A. L. (1989) in *Molecular Mechanisms of Microbial Adhesion* (Switalski, L., Hook, M., & Beachey, E., Eds.) pp 164–170, Springer-Verlag, Inc., New York.

Dabrowski, J., Houck, M., Romanowska, E., & Gamian, A. (1987) *Biochem. Biophys. Res. Commun. 146*, 1283–1285.

Davis, D. J., & Bax, A. (1985) *J. Am. Chem. Soc. 107*, 2820–2821.

Doddrell, D. M., Pegg, D. T., & Bendall, M. R. (1982) *J. Magn. Reson. 48*, 323–327.

Drickamer, K. (1988) *J. Biol. Chem. 263*, 9557–9560.

Dubois, M., Gilles, K. A., Hamilton, J. K., Rebers, P. A., & Smith, F. (1956) *Anal. Chem. 28*, 350–356.

Gronenborn, A. M., Bax, A., Wingfield, P. T., & Clore, G. M. (1989) *FEBS Lett. 243*, 93–98.

Heeb, M. J., Costello, A. H., & Gabriel, O. (1982) *Infect. Immun. 38*, 993–1002.

Heeb, M. J., Marini, A. M., & Gabriel, O. (1985) *Infect. Immun. 47*, 61–67.

Hughes, C. V., Kolenbrander, P. E., Anderson, R. N., & Moore, L. V. H. (1988) *Appl. Environ. Microbiol. 54*, 1957–1963.

Jentoft, N. (1985) *Anal. Biochem. 148*, 424–433.

Jones, C. (1985) *Carbohydr. Res. 139*, 75–83.

Kilian, M., Mikkelsen, L., & Henrichsen, J. (1989) *Int. J. Syst. Bacteriol. 39*, 471–484.

Koga, T., Okahashi, N., Yamamoto, T., Mizuno, J., Inoue, M., & Hamada, S. (1983) *Infect. Immun. 42*, 696–701.

Levitt, M. H., Freeman, R., & Frenkiel, T. (1982) *J. Magn. Reson. 47*, 328–330.

McIntire, F. C., Vatter, A. E., Baros, J., & Arnold, J. (1978) *Infect. Immun. 21*, 978–988.

McIntire, F. C., Crosby, L. K., Barlow, J. J., & Matta, K. L. (1983) *Infect. Immun. 1*, 848–850.

McIntire, F. C., Crosby, L. K., Vatter, A. E., Cisar, J. O., McNeil, M. R., Bush, C. A., Tjoa, S. S., & Fennessy, P. V. (1988) *J. Bacteriol. 170*, 2229–2235.

Morat, C., Taravel, F. R., & Vignon, M. R. (1988) *Magn. Reson. Chem. 26*, 264–270.

Muller, N., Ernst, R. R., & Wuthrich, K. (1986) *J. Am. Chem. Soc. 108*, 6482–6492.

Piantini, U., Sorensen, O. W., & Ernst, R. R. (1982) *J. Am. Chem. Soc. 104*, 6800–6801.

Rance, M., Sorensen, O. W., Bodenhausen, G., Wagner, G., Ernst, R. R., & Wuthrich, K. (1983) *Biochem. Biophys. Res. Commun. 117*, 479–485.

Redfield, A. G. (1978) *Methods Enzymol. 49*, 253–270.

Richards, J. C., Perry, M. E., & Carlo, D. J. (1983) *Can. J. Biochem. Cell Biol. 61*, 178–190.

Sato, S., Koga, T., & Inoue, M. (1984) *J. Gen. Microbiol. 130*, 1351–1357.

Shaka, A. J., Keelar, J., Frenkiel, T., & Freeman, R. (1983) *J. Magn. Reson. 52*, 335–338.

States, D. J., Hakerborn, R. A., & Ruben, D. J. (1982) *J. Magn. Reson. 48*, 286–292.

Strömberg, N., & Karlsson, K.-A. (1990) *J. Biol. Chem. 265*, 11251–11258.

Widmer, H., & Wuthrich, K. (1987) *J. Magn. Reson. 74*, 316–336.

Uhrinova, S., Petrakova, E., Ruppeldt, J., & Uhrin, D. (1990) *Magn. Reson. Chem. 28*, 979–987.